Cucurbit[8]uril–guest–metal ion self-assemblies as fluorescence sensor array for discrimination and detection of physiological phosphates

Ru–Pei Yang[a], Hong–Xue Wang[a], Qing Tang[c], Jian-Hang Hu[a], Hong-Ling Yi[d], Hong-Yuan Hu[a], Zhu Tao[a], Ying Huang[b, *]

[a]*Key Laboratory of Macrocyclic and Supramolecular Chemistry of Guizhou Province, Guizhou University, Guiyang 550025, China.*

[b]*The Engineering and Research Center for Southwest Bio–Pharmaceutical Resources of National Education Ministry of China, Guizhou University, Guiyang 550025, China*

[c]*Department College of Tobacco Science, Guizhou University, Guiyang 550025, China*

[d]*School of Pharmaceutical Sciences, Guizhou University, Guiyang 550025, China.*

Correponding e–mail: yinghung128@163.com

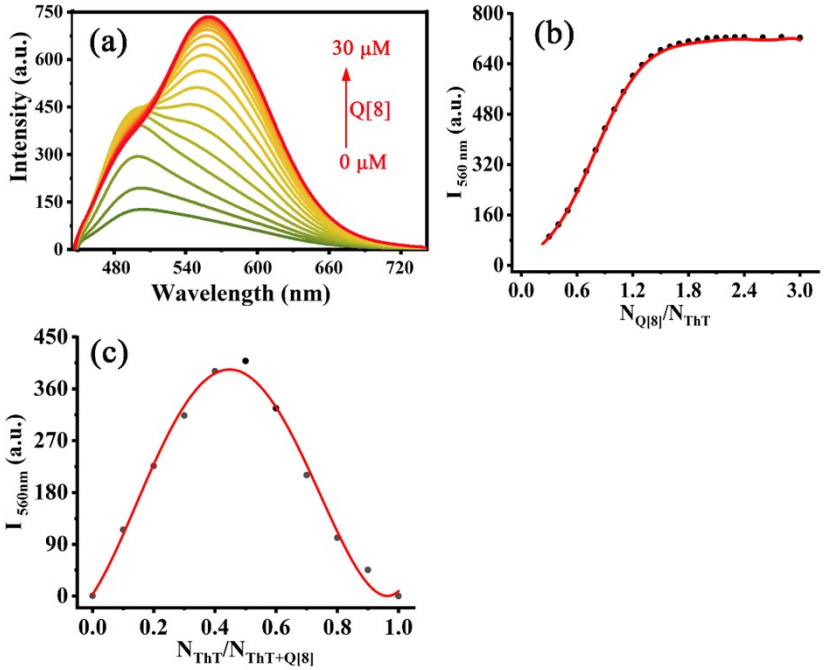

Fig. S1 The fluorescence spectra (a) and corresponding fluorescence scatter plots (b) of different

concentrations of Q[8] (0- 30 μM) added to the ThT (10 μM) solution, as well as the Jobs plot of $N_{ThT}/N_{Q[8]+ThT}$ (c).

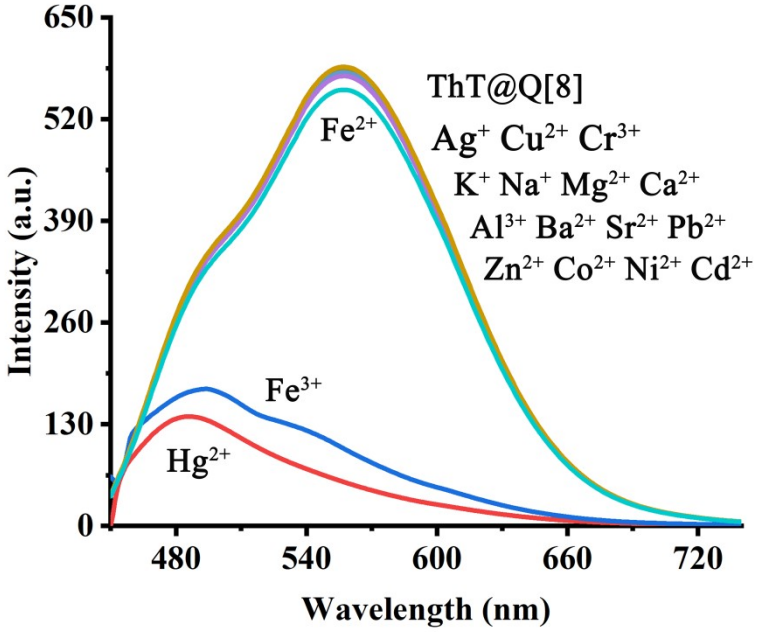

Fig. S2 The effect of M^{n+}cations (50 equiv. of host-guest complex) on the relative fluorescence response (λ_{ex}= 408 nm) of ThT@Q[8] (1:1, 10 μM) in aqueous solusion.

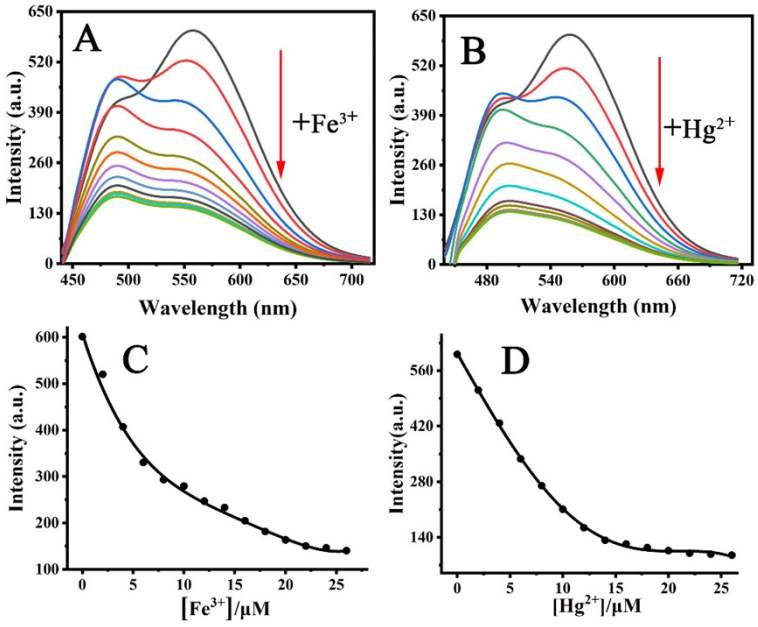

Fig. S3 The fluorescence spectra (A, B) and the corresponding I ~ $C_{Fe^{3+}/Hg^{2+}}$ curves (C, D) of Fe^{3+} and Hg^{2+} were gradually added into ThT@Q[8] solution.

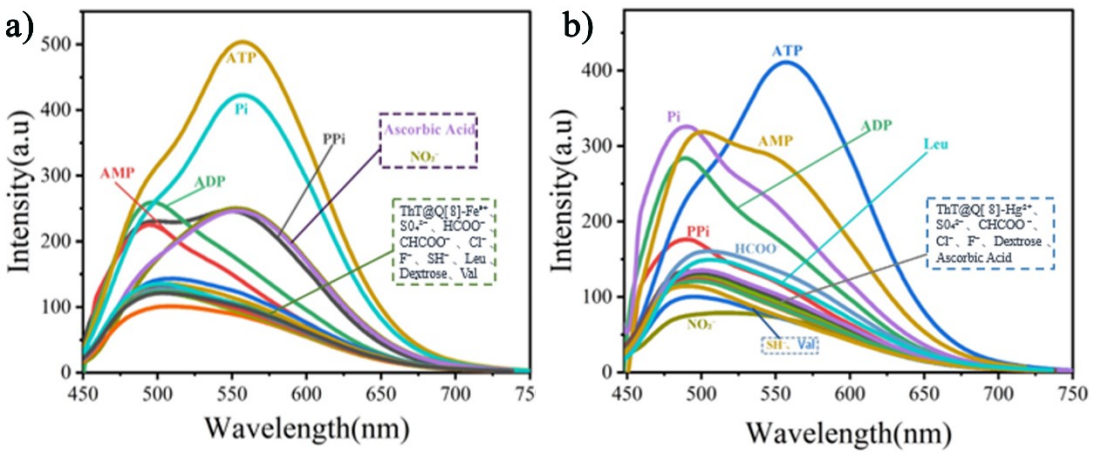

Fig. S4 Selectivity assessment of the (a) ThT-Q[8]-Fe^{3+} and (b) ThT@Q[8]-Hg^{2+} probes. The histogram shows the fluorescence response of the probes toward the five target phosphate anions (Pi, PPi, AMP, ADP, and ATP), common inorganic anions(NO_2^-, SO_4^{2-}, $HCOO^-$, CH_3COO^-, Cl^-, F^-, SH^-), and bio-relevant small molecules (valine, leucine, dextrose, ascorbic acid).

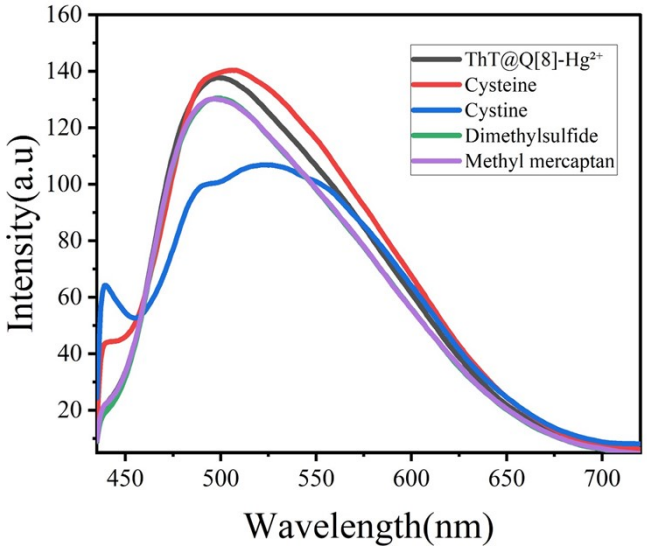

Fig. S5 The selectivity of probes ThT@Q[8]-Hg^{2+} probe towards various thiol derivatives (cystine, cysteine, methanethiol, dimethyl sulfide).

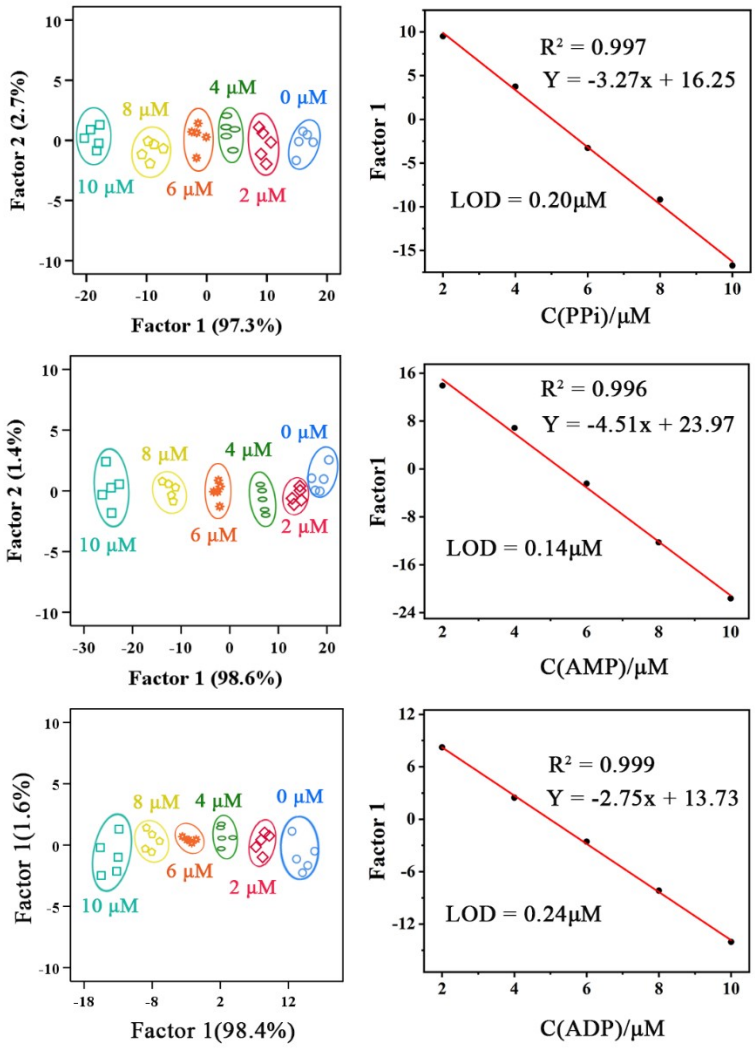

Fig. S6 Plot of LDA scores and linearity of the array sensor for different concentrations of (PPi, AMP, ADP).

(a)

ATP (μM)	Luminometer (RLU)
0	0
0.01	279
0.003	853
0.1	2270
0.3	8665
1	30908
3	86017
10	287594

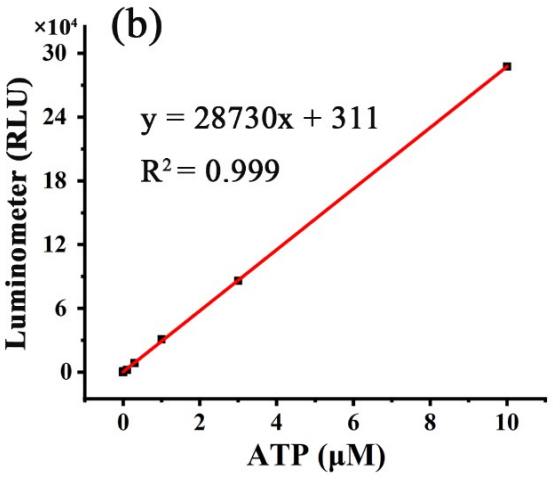

Fig. S7 The chemiluminescence and standard curve of different concentrations of ATP were detected by ATP standard kit.

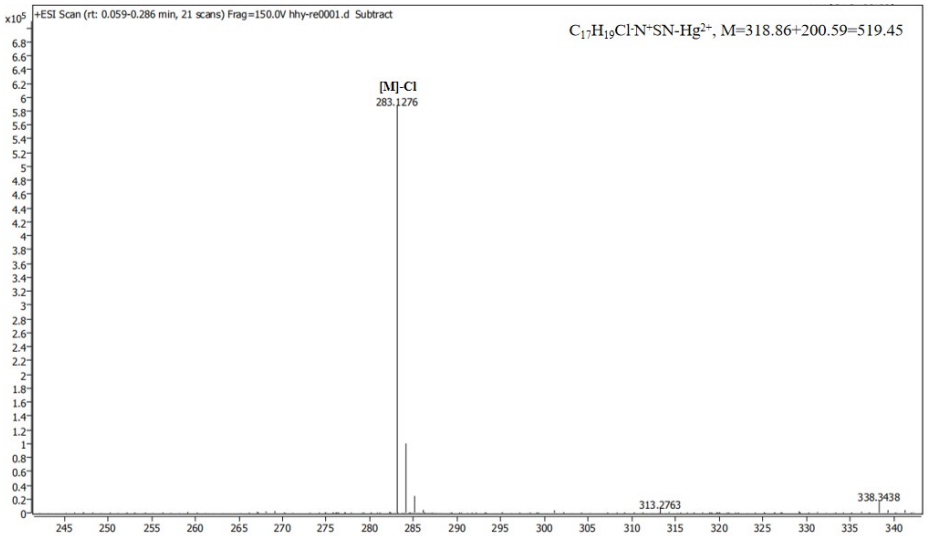

Fig. S8 Mass spectrometric analysis of the ThT and Hg^{2+} mixture.

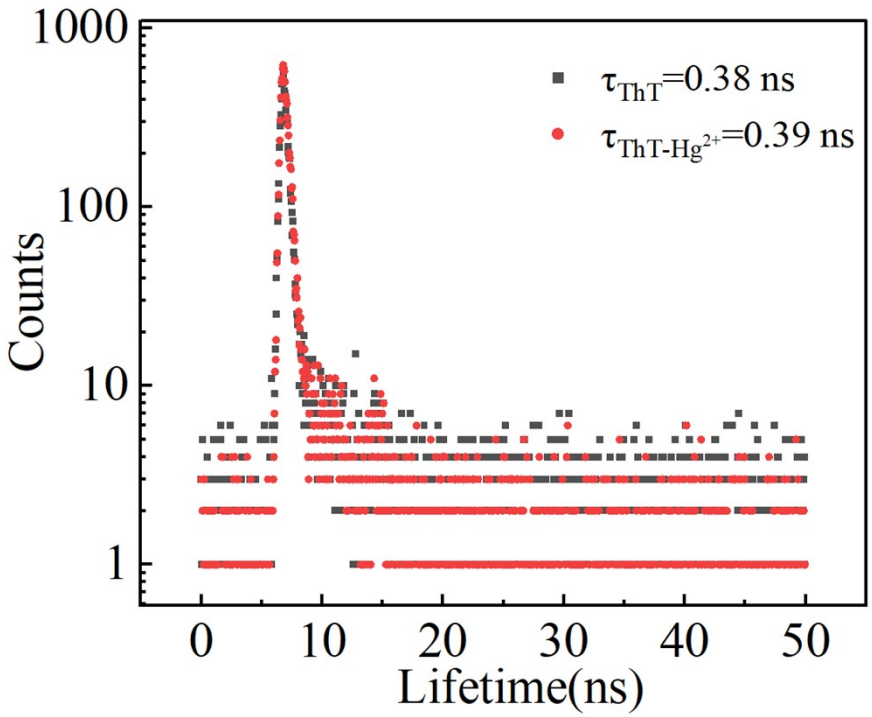

Fig. S9 Fluorescence decay profiles of ThT in the absence and presence of Hg^{2+}.

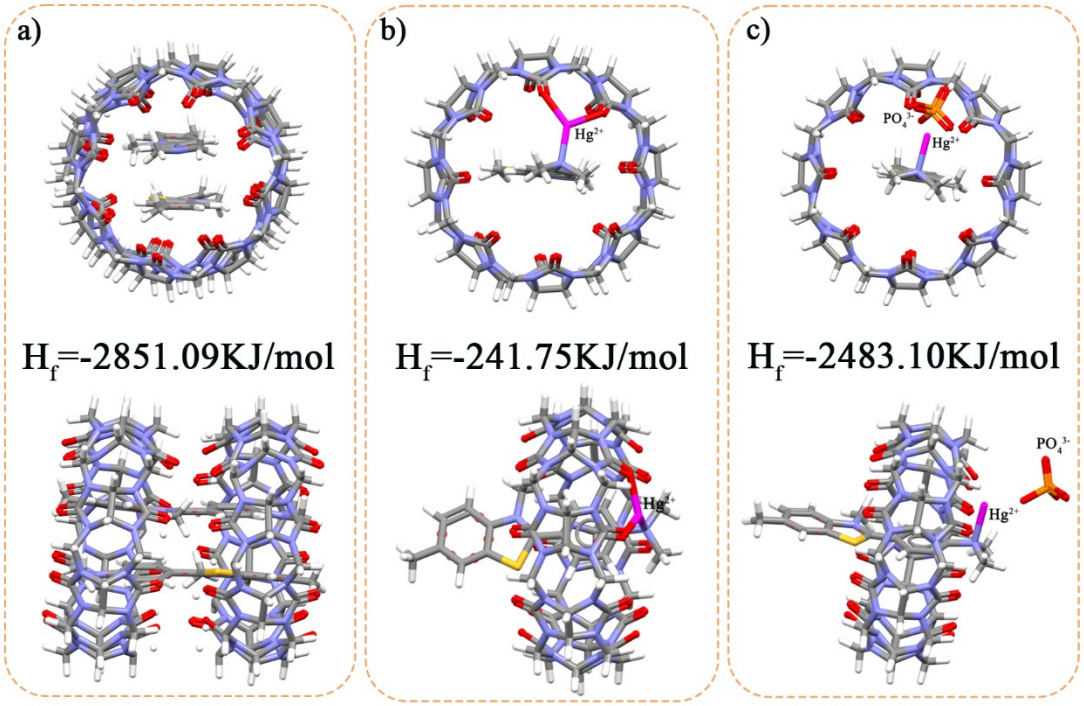

Fig. S10 DFT calculated optimized energies of three complexes, (a) ThT-Q[8]（2∶2）, (b) ThT-Q[8]-Fe^{3+}, and (c) ThT-Q[8]-Fe^{3+}-PO_4^{3-}.

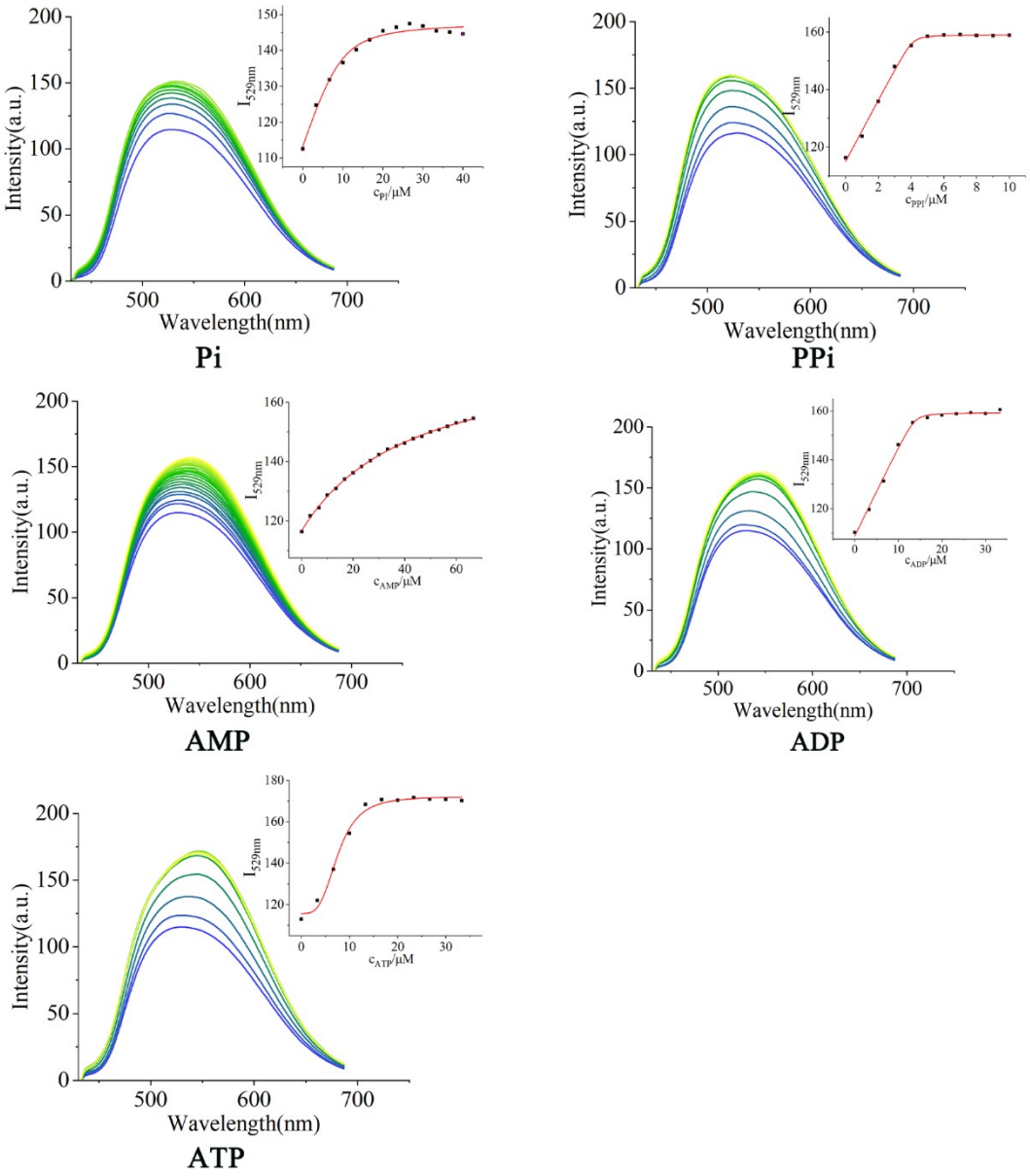

Fig. S11 Fluorescence titration spectra of ThT@Q[8]-Fe^{3+} with increasing concentrations of the five phosphate anions Pi, PPi, AMP, ADP, and ATP, respectively. The corresponding fitting curves of the fluorescence intensity change versus analyte concentration.

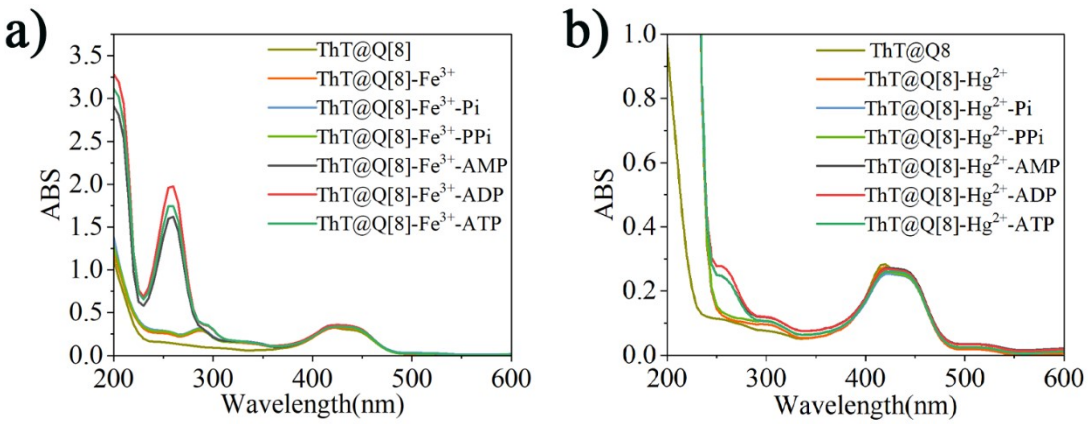

Fig. S12 UV-vis absorption spectra of (a) ThT@Q[8]-Fe^{3+} and (b) ThT@Q[8]-Hg^{2+} upon addition of various phosphate anions.

Table S1 Data for fluorescence intensity and F-value of phosphate ions (10.0 μM) detected by the fluorescence sensor array.

	Fluorescence intensity value		Convert to F-value	
	ThT@Q[8]-Fe^{3+}	ThT@Q[8]-Hg^{2+}	ThT@Q[8]-Fe^{3+}	ThT@Q[8]-Hg^{2+}
Probe	110	53	0.9736	1.0019
	97	68	1.0000	0.9739
	99	62	0.9959	0.9851
	94	55	1.0061	0.9981
	98	57	0.9980	0.9944
Pi	422	206	0.3408	0.7164
	425	203	0.3347	0.7220
	420	200	0.3448	0.7276
	424	210	0.3367	0.7090
	428	223	0.3286	0.6847
PPi	240	110	0.7099	0.8955
	245	115	0.6998	0.8862
	233	113	0.7241	0.8899
	248	110	0.6937	0.8955
	250	118	0.6897	0.8806
AMP	135	270	0.9229	0.5970
	159	265	0.8742	0.6063
	133	275	0.9270	0.5877
	136	269	0.9209	0.5989
	128	273	0.9371	0.5914
ADP	166	164	0.8600	0.7948
	175	167	0.8418	0.7892
	182	170	0.8276	0.7836
	165	169	0.8621	0.7854

	170	162	0.8519	0.7985
ATP	504	410	0.1744	0.3358
	500	408	0.1826	0.3396
	508	413	0.1663	0.3302
	517	405	0.1481	0.3451
	499	408	0.1846	0.3396

Table S2 Data for fluorescence intensity and F-value of phosphate ions (4.0 μM) detected by the fluorescence sensor array.

	Fluorescence intensity value		Convert to F-value	
	ThT@Q[8]-Fe^{3+}	ThT@Q[8]-Hg^{2+}	ThT@Q[8]-Fe^{3+}	ThT@Q[8]-Hg^{2+}
Probe	100	65	0.9939	0.9795
	97	68	1.0000	0.9739
	99	62	0.9959	0.9851
	94	67	1.0061	0.9757
	98	63	0.9980	0.9832
Pi	180	111	0.8316	0.8937
	185	115	0.8215	0.8862
	179	107	0.8337	0.9011
	186	113	0.8195	0.8899
	183	104	0.8256	0.9067
PPi	150	100	0.8925	0.9142
	157	105	0.8783	0.9049
	159	102	0.8742	0.9104
	147	106	0.8986	0.9030
	155	107	0.8824	0.9011
AMP	118	110	0.9574	0.8955
	115	116	0.9635	0.8843
	113	118	0.9675	0.8806
	117	112	0.9594	0.8918
	112	121	0.9696	0.8750
ADP	130	100	0.9331	0.9142
	135	108	0.9229	0.8993
	138	105	0.9168	0.9049
	136	106	0.9209	0.9030
	134	108	0.9249	0.8993
ATP	180	138	0.8316	0.8433
	188	130	0.8154	0.8582
	181	135	0.8296	0.8489
	195	137	0.8012	0.8451
	184	142	0.8235	0.8358

Table S3 Data for fluorescence intensity and F-value of phosphate ions (0.25 μM) detected by the

fluorescence sensor array.

	Fluorescence intensity value		Convert to F-value	
	ThT@Q[8]-Fe^{3+}	ThT@Q[8]-Hg^{2+}	ThT@Q[8]-Fe^{3+}	ThT@Q[8]-Hg^{2+}
Probe	108	65	0.9777	0.9832
	92	68	1.0101	1.0056
	105	62	0.9838	0.9720
	109	67	0.9757	0.9795
	99	63	0.9959	0.9907
Pi	130	111	0.9331	0.9347
	127	115	0.9391	0.9291
	125	107	0.9432	0.9198
	135	113	0.9229	0.9366
	121	104	0.9513	0.9142
PPi	111	100	0.9716	0.9571
	109	105	0.9757	0.9664
	105	102	0.9838	0.9534
	113	106	0.9675	0.9496
	115	107	0.9635	0.9608
AMP	124	110	0.9452	0.9179
	128	116	0.9371	0.9254
	119	118	0.9554	0.9160
	120	112	0.9533	0.9310
	122	121	0.9493	0.9235
ADP	135	100	0.9229	0.9590
	133	108	0.9270	0.9701
	138	105	0.9168	0.9664
	132	106	0.9290	0.9534
	130	108	0.9331	0.9683
ATP	109	138	0.9757	0.8769
	113	130	0.9675	0.8787
	112	135	0.9696	0.8619
	107	137	0.9797	0.8675
	105	142	0.9838	0.8731

Table S4 Leave-One-Out Cross-Validation Classification Matrix for Phosphate Anions at 10 μM.

		Predictive classification						Total
	A^{n-}	Control	Pi	PPi	AMP	ADP	ATP	
Cross-validated %	Control	5	0	0	0	0	0	100

	Pi	0	5	0	0	0	100
	PPi	0	0	5	0	0	100
	AMP	0	0	0	5	0	100
	ADP	0	0	0	0	5	100
	ATP	0	0	0	0	0	5	100

Note: The matrix is derived from the LDA model trained on the fluorescence response of the 2-sensor array to 5 replicates of each analyte. Each entry represents the percentage of replicate samples assigned to each predicted class during cross-validation. The 100% classification accuracy for all analytes demonstrates the strong discriminatory power of the sensor array, which is visually evident in the well-separated clusters in Fig. 3A.

Table S5 Leave-One-Out Cross-Validation Classification Matrix for Phosphate Anions at 4 μM

		Predictive classification						Total
	A^{n-}	Control	Pi	PPi	AMP	ADP	ATP	
Cross-validated %	Control	5	0	0	0	0	0	100
	Pi	0	5	0	0	0	0	100
	PPi	0	0	5	0	0	0	100
	AMP	0	0	0	5	0	0	100
	ADP	0	0	0	0	5	0	100
	ATP	0	0	0	0	0	5	100

Note: The matrix is derived from the LDA model trained on the fluorescence response of the 2-sensor array to 5 replicates of each analyte. Each entry represents the percentage of replicate samples assigned to each predicted class during cross-validation. The 100% classification accuracy for all analytes demonstrates the strong discriminatory power of the sensor array, which is visually evident in the well-separated clusters in Fig. 3B.

Table S6 Leave-One-Out Cross-Validation Classification Matrix for Phosphate Anions at 0.25 μM

	Predictive classification	Total

	A^{n-}	Control	Pi	PPi	AMP	ADP	ATP	
Cross-validated %	Control	5	0	0	0	0	0	100
	Pi	0	5	0	0	0	0	100
	PPi	0	0	5	0	0	0	100
	AMP	0	0	0	5	0	0	100
	ADP	0	0	0	0	5	0	100
	ATP	0	0	0	0	0	5	100

Note: The matrix is derived from the LDA model trained on the fluorescence response of the 2-sensor array to 5 replicates of each analyte. Each entry represents the percentage of replicate samples assigned to each predicted class during cross-validation. The 100% classification accuracy for all analytes demonstrates the strong discriminatory power of the sensor array, which is visually evident in the well-separated clusters in Fig. 3C.

Table S7 Reproducibility of the fluorescence response of the sensor array to four phosphate.

Sample	S1	S2	S3	S4	S5	S6	S7	S8	S9	S10	RSD(%)
Pi	-14.97	-14.81	-15.09	-15.25	-15.05	-14.82	-14.71	-15.39	-15.75	-15.05	2.94
PPi	15.25	14.99	14.42	15.46	14.87	16.20	15.00	15.32	15.46	15.42	4.46
ADP	2.23	2.54	1.97	2.28	2.04	2.54	2.77	2.07	2.29	2.64	2.59
AMP	12.28	12.80	12.70	12.43	13.00	12.58	13.40	12.70	12.43	12.39	3.17
ATP	-52.87	-52.21	-53.29	-52.34	-52.12	-52.71	-52.43	-53.09	-52.34	-52.12	3.96

Table S8 Evaluate the photostability of the fluorescence sensor array.

Analyte	Time/h	$I-I_0/I_1-I_0$	
		P1	P2
Pi	6h	0.4918	0.7983
	12h	0.4867	0.7799
	24h	0.5150	0.7711
	48h	0.5156	0.9479
	96h	0.5622	0.9823
PPi	6h	0.2870	0.8399
	12h	0.3295	0.8568
	24h	0.4078	0.8573

	48h	0.5812	1.0152
	96h	0.6752	1.0378
	6h	0.9171	0.7403
	12h	0.8873	0.4065
AMP	24h	0.8816	0.3035
	48h	0.8436	-0.0534
	96h	0.8373	-0.3246
	6h	0.8149	0.8151
	12h	0.7969	0.6380
ADP	24h	0.7948	0.5748
	48h	0.7835	0.3738
	96h	0.7792	0.1246
	6h	0.6436	0.8258
	12h	0.6517	0.7108
ATP	24h	0.6625	0.6828
	48h	0.6488	0.5263
	96h	0.6758	0.3854

Table S9 The product information of the human serum used in this study

Test	Specification
Appearance (Color)	Colorless to Brown-Yellow to Brown
Appearance (Form)	Liquid
pH	6.5-8.0
Total Protein	4.0-9.0 g/dl
Sodium (Na)	100-200 mmol/L
Iron	35-100 ug/g
Storage Temperature	-20℃

Table S10 The response of the sensing array to five phosphate anions (10 μM) in serum.

		Predictive classification						
								Total
	A^{n-}	Control	Pi	PPi	AMP	ADP	ATP	
Cross-validated %	Control	5	0	0	0	0	0	100
	Pi	0	5	0	0	0	0	100
	PPi	0	0	5	0	0	0	100
	AMP	0	0	0	5	0	0	100
	ADP	0	0	0	0	5	0	100

ATP	0	0	0	0	0	5	100

Table S11 The chemiluminescence value and ATP content of ATP in human serum at different time detected by standard kit.

	0 h	1 h	3 h	5 h	6 h
Chemiluminescence	287036	126723	103739	52025	46279
level of ATP (μM)	10	4.4	2.7	0.8	0.6
Reaction proportion	0	56%	73%	92%	94%
The remaining proportion	100%	44%	27%	8%	6%

Table S12 Binding constants of ThT@Q[8]-Fe^{3+}] for five phosphates

Sensor	K_{sv} (M^{-1})				
	ATP	ADP	AMP	PPi	Pi
ThT@Q[8]-Fe^{3+}	9.69×10^{6}	1.28×10^{6}	2.29×10^{3}	9.14×10^{5}	6.86×10^{4}

Table S13 Comparison of sensor array with other methods for detecting phosphate

Method (array)	Sensor unit	Detection limit / μM	Ref
phosphorescence	9	10	[1]
fluorescence	3	10	[2]
colorimetric	3	10	[3]
fluorescence	2	5	[4]
fluorescence	2	0.25	This work

Reference

1. H. W. He, C. H. Li, Y. F. Tian, P. Wu and X. D. Hou, *AnaCh*, 2016, **88**, 5892-5897.
2. S. Sun, K. Jiang, S. Qian, Y. Wang and H. Lin, *AnaCh*, 2017, **89**, 5542-5548.
3. L. Qin, X. Wang, Y. Liu and H. Wei, *AnaCh*, 2018, **90**, 9983-9989.
4. S. Z. Du, Z. Sun, L. Han, M. Qing, H. Q. Luo and N. B. Li, *Sensors Actuators B: Chem.*, 2020, **324**, 128757.